Vokasi Unesa Bulletin of Engineering, Technology and Applied Science (VUBETA)
https://journal.unesa.ac.id/index.php/vubeta
Vol. 2, No. 3, 2025, pp. 558~580 DOI: 10.26740/vubeta.v2i3.39071
ISSN: 3064-0768

Power Quality Enhancement Using Single Phase Shunt Active Filter Based ANFIS Supplied by Photovoltaic

Anis Fitriani[1], Amirullah[2*], Krischonme Bhumkittipich[3]
[1,2]Departement of Electrical Engineering, Faculty of Engineering, Universitas Bhayangkara Surabaya, Surabaya, Indonesia
[3]Department of Electrical Engineering, Faculty of Engineering, Rajamangala University of Technology Thanyaburi (RMUTT), Pathum Thani, Thailand

Article Info

Article history:

Received February 26, 2025
Revised July 5, 2025
Accepted July 22, 2025

Keywords:

ShAF
ANFIS
Harmonics
Reactive Power Compensation
PV

ABSTRACT

This paper proposes a single-phase shunt active filter (ShAF) combined with photovoltaic (PV) to enhance power quality performance by reducing source current harmonics and compensating for reactive power in a single-phase 220-Volt distribution system with a frequency of 50 Hz connected to a non-linear load. The PV panel consists of several PV modules with a maximum power of 600 W each. An adaptive neuro-fuzzy inference system (ANFIS) controls the voltage in the DC link capacitor circuit in the ShAF. This method is proposed to overcome the weakness of the Fuzzy Sugeno method in neural-network-based learning capabilities to determine the fuzzy rules of the input membership functions (MFs) and the weakness of the proportional-integral (PI) control in determining proportional and integral constants using trial and error method. The single-phase system is connected to a non-linear load with a combination, i.e. without ShAF, using ShAF, and using ShAF-PV, respectively, with a total of seven cases. Based on the three proposed control methods and model configurations, the ShAF-PV circuit with ANFIS control is able to result in the best performance because it is able to produce the lowest source current THD. The single-phase system using ShAF-PV with ANFIS control is also capable of injecting the largest reactive power compared to the ShAF and ShAF configurations with PI and Fuzzy-Sugeno control. The increase in reactive power in the ShAF-PV is further able to compensate for the reactive power, so it is able to suppress and reduce the source reactive power significantly.

1. INTRODUCTION

The adoption of numerous modern devices with non-linear loads in the business and residential sectors indicates an increase in electricity consumption. Power quality issues are worsening due to domestic expenses, including washing machines, televisions, air conditioners, computers, laptops, uninterruptible power supply (UPS) equipment, battery chargers, switch-mode power supplies, and refrigerators, as well as industrial expenses such as arc furnaces, metal, and paper mills. The use of rooftop solar-based independent generators with inverters by many consumers can cause source current distortion, in addition to producing power and reducing power consumption. All the equipment types can introduce harmonics into the source current, lower the power factor, and result in unbalanced loads in the distribution system. The use of intelligent control in power electronic equipment, on the other hand, also enhances the functionality of power electronic devices. Still, it introduces harmonics and distorts the waveforms of source voltages and load currents. Therefore, the regulation of low-voltage distribution systems must pay close attention to the elimination of harmonics. A ShAF, a power electronic converter-based device, was developed to improve the system's power quality and address this issue [1]. With the harmonic load linked in parallel, the ShAF injects a compensatory current that is supposed to cancel the harmonics.

*Corresponding Author
Email: amirullah@ubhara.ac.id

Numerous studies have examined the ShAF control method as a current control for non-linear loads and unbalanced currents. According [2], the P-Q and P-Q-R approaches have been used to compare the effects of system voltage on a ShAF. To reduce harmonic currents and account for reactive power, a three-phase four-wire ShAF has been developed [3]. A proposed optimal control strategy for a three-phase active filter has been presented [4]. Super twisting-sliding mode control (ST-SMC)-based space vector modulation (SVM)-based direct power control of ShAF has been introduced [5]. The fuzzy logic control-based optimization of ShAF parameters has been described [6]. On a distorted power grid, simulations and tests of the fast repetitive control (FRC) approach with closed harmonic correction for a three-phase ShAF and four-wire system have been conducted [7]. To utilize dc-link voltages, three techniques for adaptive change of dc-link voltage on shunt active filters have been compared [8].

Several researchers have suggested PV to enhance ShAF's effectiveness in improving power quality. PV-based SAPF contributes to the grid's power supply and enhances power quality during the day when sunlight is available; however, at night and when there is no sunlight, the grid is the sole source of electricity. During this time, reactive power can be compensated for, and harmonic currents can be reduced through the combination of ShAF and PV [9]. With parameter choices based on flower pollination methods, the control implementation of the Kalman Filter on a PV-connected shunt active filter has been constructed [10]. The process of balancing current and voltage due to distributed generation (DG) in the form of a single-phase PV generating unit deployed haphazardly on a three-phase, four-wire grid using battery energy storage (BES) and a single-phase bidirectional inverter [11].

For a single-phase, two-stage converter using a PV-based ShAF, the effectiveness of the two control strategies has been compared [12]. Five-stage, three-phase, disconnected, and grid-connected H-bridge models for the PV-connected DC-DC converter and shunt active filter have been created [13]. Investigations have been conducted on the PV system connected to the distribution network utilizing a two-stage circuit and a ShAF with hysteresis control [14]. It has been applied to supply active shunt filters to PV linked to the grid and controlled by digital signal processing (DSP) [15]. Using a diphase artificial neural network control approach, confirmed by the d-q reference frame method, a simulation of a PV array-based multifunctional shunt active power filter (PV-SAPF) has been conducted [16].

To eliminate source current harmonics, an adaptive hybrid energy generation system based on PV-Wind-Fuel Cell has been proposed, combined with a synchronous reference frame (SRF)- based active power filter (SAPF) [17]. To reduce harmonic currents and improve power factor correction (PFC), a distribution static compensator (D-STATCOM) without a capacitor, based on a matrix converter (MC) and operating using a finite control set-model predictive control (FCS-MPC), has been developed [18]. Grid-connected PV/wind hybrid systems have been presented and validated using the PI, Fuzzy, and ANFIS methodologies to mitigate power quality issues (sags, swells, and harmonics) by employing a distributed power flow controller (DPFC) with coordinated PQ theory and a FOPID controller [19]. A three-phase active power filter (APF) coupled to a PV panel utilizing a direct power control (DPC) technique has been researched for improved power quality [20]. With fuzzy logic control in maximum power point tracking (MPPT), this model was utilized to reduce harmonic currents caused by nonlinear load currents while simultaneously ensuring the delivery of a portion of the load request from the PV panel.

A three-phase, three-wire ShAF structure connected to the grid with a photovoltaic generator, without a DC/DC converter to compensate for harmonic currents, unbalanced currents, and reactive power, has been designed by [21]. The ShAF design, aimed at improving power quality and reducing harmonic effects resulting from the integration of PV generators into the distribution network, has been simulated [22]. The neural instantaneous power theory (Neural-IPT) based on a feed-forward backpropagation artificial neural network (FFBP-ANN), for a three-phase SAPF combined with a PV, has been implemented [23]. Power quality improvement using ShAF in grid-connected PV generation systems has been proposed [24]. Grid-connected solar systems comprise PV systems, DC-to-DC converters, batteries, three-phase inverters, power electronics devices, and non-linear loads. A PV-fed active power filter model has been designed to reduce harmonic distortion and improve the power quality of a sinusoidal alternating current supply, utilizing Internet of Things (IoT) devices [25]. An artificial intelligence method is used to generate a reference current signal and a switching signal to decide the switching status of ShAF. The improvement of the current network quality influenced by nonlinear loads supplied by a single-phase photovoltaic system connected to the grid has been investigated [26]. The improvement in energy quality produced by the grid-connected PV system, which compensates for harmonic currents due to nonlinear loads, has been observed using ShAF with multilayer feedforward neural and fuzzy logic control [27]. The use of active power filters to improve power quality in a three-phase power grid having a grid-connected bidirectional solar inverter and nonlinear loads has been investigated [28]. PV Battery System Operating in Separate and Grid-Connected Mode with Shunt Active Filter Capability has been studied [29]. Modelling of reactive power compensation using renewable energy from sunlight through photovoltaics to reduce harmonics in the electricity network using ShAF has been simulated [30].

The use of solid oxide fuel cells (SOFC) as hybrid power generators and ShAF to compensate for current harmonics has been simulated [31]. The implementation of ShAF has been observed to minimize the harmonics introduced by inverters connected to stand-alone photovoltaic solar systems and grid-connected solar systems [32]. The implementation of ShAF for harmonic mitigation in grid-integrated photovoltaic generation systems has been observed [33]. The implementation of ShAF to reduce DC-link ripple current caused by the power converter, thereby improving the life of aluminium electrolytic capacitors, has been simulated [34]. Modelling of a two-stage solar PV system integrated with ShAF for harmonic mitigation, power factor correction, and load compensation has been implemented [35]. The ShAF system is built with a three-leg Voltage Source Converter and DC power extracted from the PV modules.

The SAPF has been developed using a double buck half-bridge converter (DBHB) and a three-phase half-bridge interleaved buck shunt active power filter (HBIB-SAPF) [36][37]. An inner loop and an outer loop are present in both models. The deep loop can resolve the overshoot transition issues with various switching operating modes that occur in typical inverter circuits, in contrast to the HBIB model. The inner loop in the DBHB model serves as a single power factor control. Fuzzy logic control is used in both the HBIB and DBHB equations to maintain the DC converter voltage within the desired value range. Using a tiny capacity capacitor, a modified extraction technique has been developed [38]. The disadvantage of the traditional extraction approach is that it is sensitive to the quality of the DC-link voltage, necessitating the selection of expensive, massive capacitors with poor dynamic response and low even-order harmonic components. This approach utilizes a single-frequency-decoupled (SFD) structure with proportional-resonant (PR) control and a second-order integrator frequency-locked loop (SOGI-FLL) to decrease the size of the DC-link capacitor and minimize the SOGI-FLL. It has been noted that PV systems with PV panels, half-bridge inverters with capacitive dividers, and LCLs coupled to a single-phase grid exhibit nonlinear modelling and control [39].

To regulate a SAPF with three-phase, reduced-connected PV panels, a controller design method based on an automated hybrid approach was developed [40]. This approach uses an inner loop control and an outer loop control, two cascade loop controllers. Deep loop control is utilized to ensure that the switching design's operational model can produce an input power factor of 1. While the MPPT perturb and observer (P and O) are utilized to manage the PV panel output voltage using a PI regulator in the outer loop (P and O). In a separate investigation, a half-bridge inverter was coupled to two PV arrays via a single-phase SAPF controller and two DC-link capacitors [41]. To achieve an input power factor of one and account for harmonic and reactive currents caused by nonlinear loads, the inner loop is designed differently from the previous method, utilizing the sliding mode method and the Lyapunov stability methodology. Also contains an adaptive observer for an online estimate of variables related to the grid state that are not measurable. The PV output voltage is controlled using an incremental conductance (IC) algorithm in the outer loop, which mainly consists of a filtered PI regulator, to attain the MPPT value. Additionally, by adjusting the DC capacitor voltage, the power exchange between the PV source and the AC power grid can be balanced.

The use of PV-based ShaF to improve power quality using the P-Q theory method has been simulated [42]. Mapping of instantaneous load and source characteristics has been proposed [43] for a solar interface front-end inverter operating as a ShAF, as well as an active power injector, to accommodate the dynamic variations of source and load. A three-level Neutral Point clamped (NPC) photovoltaic (PV) interface voltage source inverter based on three-phase Shunt Active Power Filter (SAPF) has been proposed [44]. The proposed system is capable of compensating reactive power, minimising source current THD, improving power factor, and injecting PV system energy into the power system. The implementation of ShAF based on PV connected to storage devices has been simulated [45]. The proposed model can generate and inject maximum PV power into the system, ensuring that the grid current remains healthy by offering high filtering quality at the grid side. The use of an adaptive method in controlling two-stage PV-based ShAF under distorted grid conditions and stochastic PV system behaviour has been proposed [46]. A compact structure, a shunt active photovoltaic filter based on cascaded H-bridge multilevel inverter (SAF-PV/CHB-MLI) to eliminate electrical disturbances caused by nonlinear loads and to generate MPPT from PV generator has been proposed [47].

The research proposes a ShAF combined with PV to reduce source current harmonics and compensate for reactive power in a single-phase distribution system connected to a non-linear load. The ANFIS method controls the voltage in the DC link capacitor circuit in the ShAF. This method was further validated using fuzzy logic control with the Sugeno-Fuzzy Inference System (FIS) method, also referred to as the Fuzzy-Sugeno method and the PI method, to determine the effectiveness and optimal performance of the proposed method. Referring to the problems above, the main contributions of this research are:

1. Design a ShAF model supplied by PV and then implement the single-phase ShAF-PV configuration in a single-phase low-voltage distribution system to reduce source current harmonics and compensate for reactive power due to non-linear loads. The ShAF circuit is located between the load bus and the source bus (PCC), which is then connected to a single-phase 220 V distribution line with a frequency of 50 Hz. The PV panel consists of several PV modules with a maximum power of 600 W.

2. Validate the performance of the single-phase ShAF-PV configuration against the single-phase ShAF configuration to determine the optimal system configuration for mitigating source current harmonics and compensating reactive power resulting from the contribution of non-linear loads on a 220 V single-phase low-voltage distribution line.
3. Implement ANFIS control methods in single-phase ShAF-PV and single-phase ShAF, respectively, to overcome the weaknesses of the Sugeno Fuzzy Method in neural-network-based learning capabilities to determine fuzzy rules from input membership functions (MFs) as well as weaknesses in PI control in determining proportional gain (K_p) and integral gain (K_I) in the proposed model.
4. Validate the results of the ANFIS control method using the Fuzzy-Sugeno and PI methods on single-phase ShAF-PV and single-phase ShAF circuits to determine the best control system performance in mitigating source current THD and compensating reactive power when the system is connected to a non-linear load.

The structure of this article is as follows: Chapter 2 presents the proposed method, Chapter 3 discusses the results and conclusions, and Chapter 4 provides the conclusion.

2. METHOD

2.1. Proposed Method

This paper proposes a single-phase ShAF model supplied by PV (ShAF-PV) to mitigate source current harmonics and compensate for load reactive power in distribution lines connected to non-linear loads. The performance of source current harmonics and reactive power compensation was tested using two circuit combinations: single-phase ShAF and single-phase ShAF-PV. The PV panel consists of several PV modules, each with a maximum power of 600 W. There are three proposed power electronics devices, namely ShAF one phase and single phase ShAF-PV. The ShAF-PV system is proposed to overcome the weakness of the ShAF circuit in reactive power compensation, thereby mitigating source current harmonics in a single-phase connected distribution system with non-linear loads. The ShAF-PV circuit is located between the load bus and is connected to the source bus or point common coupling (PCC) via a single-phase 220 V low-voltage distribution line with a frequency of 50 Hz. The ANFIS controller is proposed to overcome the weakness of the Fuzzy-Sugeno method in neural-network-based learning capabilities to determine the fuzzy rules of the input MFs and the weakness of the PI method in determining proportional gain (K_p) and integral gain (K_I). The proposed model of a single-phase ShAF-PV system is presented in Figure 1.

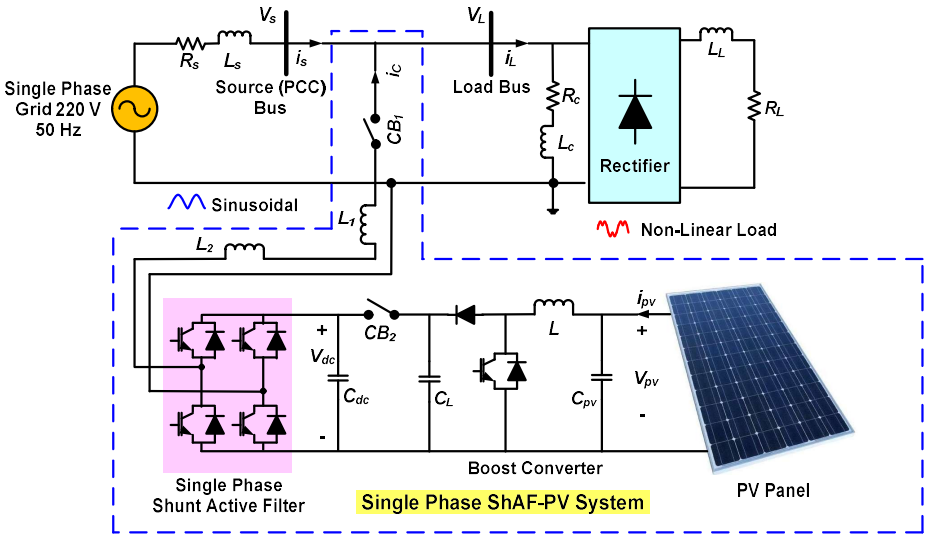

Figure 1. Proposed model of a single-phase ShAF-PV system connected to a non-linear load

ANFIS control is implemented as a DC voltage control on a single-phase ShAF to reduce source current harmonics and compensate for reactive power, and then the results are compared with FS control and PI control. In the configuration of the ShAF model and the ShAF-PV model, each proposed configuration utilizes PI, FS, and ANFIS controls, resulting in a total of six cases. The results of the analysis were carried out on the parameters, namely the magnitude and THD of the current on the source bus, the magnitude and THD of the current on the load bus, the magnitude and THD of the ShAF current, the reactive power of the source, the active power of the load, and the reactive power of the ShAF. The current flowing from the ShAF to the single-phase distribution line is then known as the shunt compensation current. Meanwhile, the reactive power flow

from ShAF, hereinafter referred to as shunt reactive power compensation, functions to suppress and reduce the reactive power of the source. After all, parameters are obtained, the next step is to determine the best combination of ShAF circuits and control methods in reducing source current harmonics and compensating for reactive power. Figure 2 shows the active and reactive power flows using a circuit without ShAF, ShAF, and ShAF-PV in a single-phase system connected to a non-linear load. The simulation parameters for the proposed model are further shown in Table 1.

Table 1. System Parameters

Devices	Parameters	Values
Single Phase Grid	RMS Voltage Frequency Line Impedance	220 Volt 50 Hz R_S = 1 Ω L_S = 1 mH
Shunt Active Filter	Shunt Inductance	L_{Sh} = 1.5 mH
Non-Linear Load	Resistance Inductance Load Impedance	R_L = 57 Ω L_L = 0.5 mH R_C = 60 ohm, L_C = 0.5 mH
DC Link	DC Voltage Capacitance	V_{dc} = 650 volt C_{dc} = 3000 µF
Photovoltaic Panel	Active Power Irradiance Temperature MPPT	0.6 kW 1000 W/m2 25^0 C Perturb and Observe
Proportional Integral Parameter	Proportional Gain (K_P) Integral Gain (K_I)	K_P=0.2 K_I=1.5
Fuzzy Logic Controller	Fuzzy Inference System Composition Defuzzyfication	Sugeno Max-Min Wtaver
Input Memberships Function	Error V_{dc} ($V_{dc-error}$) Delta Error V_{dc} ($\Delta V_{dc-error}$)	trapmf and trimf trapmf and trimf
Output Membership Function	Instantaneous of Power Losses ($\tilde{p}_{loss}$)	constant [0,1]
ANFIS Training Method	Neural Network Algorithm	Backpropagation
ANFIS Maximum Iteration	Epoch	40
ANFIS Training Error	Error Degree	0

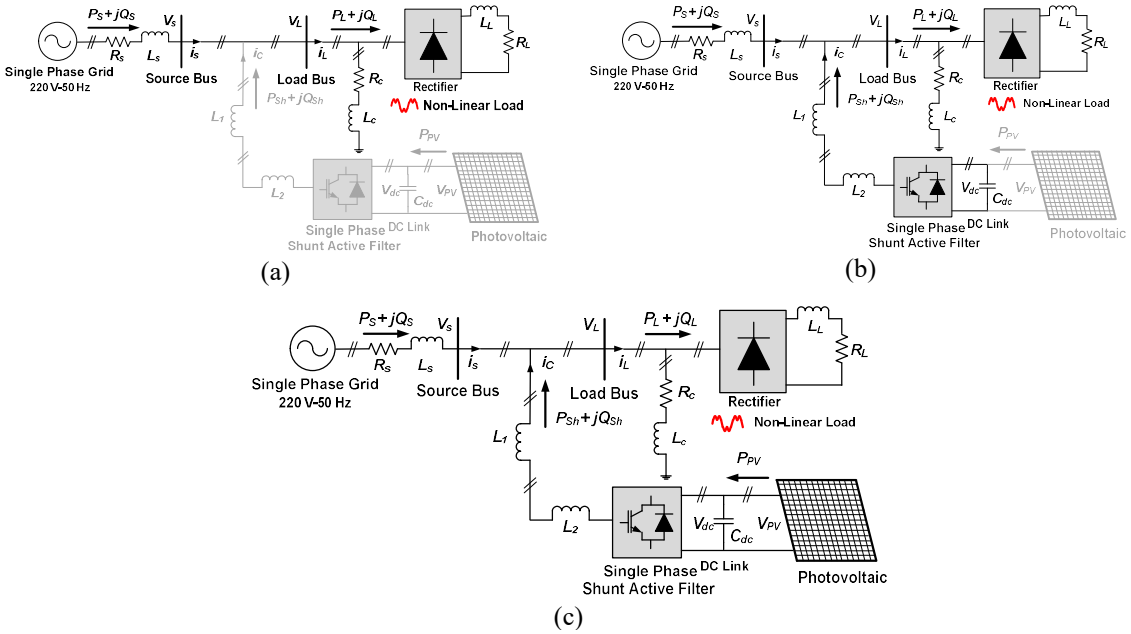

Figure 2. Active and reactive power transfer of the circuit (a) Without ShAF, (b) ShAF,

(c) ShAF-PV in a single-phase system connected to a non-linear load

The study uses three model configurations in Figure 2a, Figure 2b, and Figure 2c, with seven cases each described as follows:

1. Case 1 (Without ShAF), In this case, the system is connected to an NL load, a sinusoidal source, without using ShAF.
2. Case 2 (With ShAF-PI), In this case, the system is connected to an NL load, a sinusoidal source, and uses ShAF with PI control.
3. Case 3 (With ShAF-FS), In this case, the system is connected to an NL load, sinusoidal source, and uses ShAF with FS control.
4. Case 3 (With ShAF-ANFIS), In this case, the system is connected to an NL load, a sinusoidal source, and uses ShAF with ANFIS control.
5. Case 4 (With ShAF-PV-PI), In this case, the system is connected to an NL load, sinusoidal source, and using ShAF supplied PV with PI control.
6. Case 5 (With ShAF-PV-FS), In this case, the system is connected to an NL load, sinusoidal source, and using ShAF is supplied with PV with FS control.
7. Case 6 (With ShAF-PV-ANFIS), In this case, the system is connected to an NL load, sinusoidal source, and using ShAF supplied PV with ANFIS control.

2.2. Single-Phase Shunt Active Filter Control Using PQ Theory

Due to its well-known topology and simple installation process, the ShAF type is the most popular. The basic design of an active power filter in parallel with a voltage source inverter (VSI) is depicted in Figure 1. It consists of a capacitor acting as the terminal (C_{dc}), four insulated-gate bipolar transistors (IGBTs) acting as a power electronics switch, and two inductors (L_1 and L_2) acting as an interfacing component [9]. The fundamental idea behind ShAF is to inject a compensation current (I_c) whose phase is inversely proportional to the phase of the harmonic load current (I_L). The vector sum of the source current (I_S). The source bus or PCC bus will be close to zero when the compensation current and load harmonic current have the same or opposite phases at the harmonic frequency, resulting in the nearly sinusoidal current waveform depicted in Figure 1. The ShAF is arranged parallel to the grid in the application. The ShAF measures the current, voltage, and DC-link capacitor (C_{dc}), on the load side, to produce a reference signal. A reference harmonic is created using the current signal and is later reversed. The power factor is improved by using the voltage signal in such a way that the grid current supply is in phase with the grid voltage. Through the PCC bus, the processing circuit's output signal is utilised to regulate switching on the inverter connected to the grid in parallel.

The ShAF circuit is made up of an active filter, a non-linear load, and an AC source voltage (V_S). The source current (I_S), which flows in the direction of the non-linear load, powers the load. The line from the active filter branches between the source bus and the nonlinear load. This line offers an inverter current that reduces harmonics and accounts for reactive power so that the source current's (I_S) power factor and harmonic values can satisfy IEEE 519 requirements. Due to the influence of switching power electronic circuits and the huge reactive power devices of non-linear loads, the load current (I_L) still exhibits harmonics and a low power factor. For three-wire, three-phase power systems, as well as three-phase, four-wire power systems, the p-q theory, also known as instantaneous power theory, is frequently employed. This theory employs three voltage and current signals, but it can also be applied to single-phase active filters by duplicating two more voltage and current signals with a 120º angle shift. The foundation of this theory is the division of power components into mean and oscillations. Assign phase "a" to the load current of a single-phase load, and phases "b" and "c" to the duplicating technique's additional phases. Mathematically, the load current can be expressed as phase current "a" using the Equation. (1). By assuming that Equation (1) represents the load current for the phase "a," Equations (2) and (3) below can be used to describe the load current for phases "b" and "c" [48].

$$i_a = \sum_{i=0}^{n} \sqrt{2}\, I_i \sin(w_i + \theta_i) \quad (1)$$

$$i_b = \sum_{i=0}^{n} \sqrt{2}\, I_i \, sin\, (w_i + \theta_i - 120°) \quad (2)$$

$$i_c = \sum_{i=0}^{n} \sqrt{2}\, I_i \sin\, (w_i + \theta_i - 120°) \quad (3)$$

By assuming that Equation (1) represents the load current for the phase "a," Equations (2) and (3) below can be used to describe the load current for phases "b" and "c." [48].

$$\begin{bmatrix} i_a \\ i_b \\ i_c \end{bmatrix} = \begin{bmatrix} 1 \\ 1\angle 120° \\ 1\angle 240° \end{bmatrix} [i_a] \quad (4)$$

$$\begin{bmatrix} v_a \\ v_b \\ v_c \end{bmatrix} = \begin{bmatrix} 1 \\ 1\angle 120° \\ 1\angle 240° \end{bmatrix} [v_a] \quad (5)$$

Use Equation (6) for load current and Equation (7) for load voltage to calculate the α dan β reference currents and the Clarke transformation [48].

$$\begin{bmatrix} i_\alpha \\ i_\beta \\ i_o \end{bmatrix} = \sqrt{\frac{2}{3}} \begin{bmatrix} 1 & -\frac{1}{2} & \frac{1}{2} \\ 0 & \frac{\sqrt{3}}{2} & -\frac{\sqrt{3}}{2} \\ \frac{1}{\sqrt{2}} & \frac{1}{\sqrt{2}} & \frac{1}{\sqrt{2}} \end{bmatrix} \begin{bmatrix} i_a \\ i_b \\ i_c \end{bmatrix} \quad (6)$$

$$\begin{bmatrix} v_\alpha \\ v_\beta \\ v_o \end{bmatrix} = \sqrt{\frac{2}{3}} \begin{bmatrix} 1 & -\frac{1}{2} & \frac{1}{2} \\ 0 & \frac{\sqrt{3}}{2} & -\frac{\sqrt{3}}{2} \\ \frac{1}{\sqrt{2}} & \frac{1}{\sqrt{2}} & \frac{1}{\sqrt{2}} \end{bmatrix} \begin{bmatrix} v_a \\ v_b \\ v_c \end{bmatrix} \quad (7)$$

According [48], the active and reactive powers are expressed as Equation (8), Equation (9), and Equation (10) respectively:

$$p = v_a i_a + v_\beta i + v_o i_o \quad (8)$$

$$q = v_a i_a - v_\beta i_\beta \quad (9)$$

$$\begin{bmatrix} p \\ q \end{bmatrix} = \begin{bmatrix} v_\alpha & v_\beta \\ -v_\beta & v_\alpha \end{bmatrix} \begin{bmatrix} i_\alpha \\ i_\beta \end{bmatrix} \quad (10)$$

The two portions that make up active and reactive power are the average and oscillating, or the DC section and the AC section, respectively. The equations for both active and reactive power are as follows:

$$p = \bar{p} + \tilde{p}$$
$$q = \bar{q} + \tilde{q}$$

A low-pass filter, which may eliminate high frequencies and yield a fundamental component or DC section, can be used to determine the DC section. Equation (11) can be used to describe the α-β reference current in terms of the part's DC active power and reactive power [49].

$$i^*_{\alpha\beta} = \frac{1}{v_\alpha^2 + v_\beta^2} \begin{bmatrix} v_\alpha & v_\beta \\ v_\beta & -v_\alpha \end{bmatrix} \begin{bmatrix} -\tilde{p} + \bar{p}_{loss} \\ -q \end{bmatrix} \quad (11)$$

Average active power is derived using the $\bar{p}_{loss}$ parameter from the voltage controller. Before the signal is reduced to the load current, the active power filter's three-phase reference current is given in Equation (12). The pulse width modulation (PWM) signal is created utilizing the hysteresis band and the reduced three-phase current. Only two of the six PWM signals produced by the hysteresis band are used as the hysteresis band input for a single-phase active filter [48].

$$i^*_{abc} = \sqrt{\frac{2}{3}} \begin{bmatrix} 1 & 0 \\ -1/2 & \sqrt{3}/2 \\ -1/2 & -\sqrt{3}/2 \end{bmatrix} i^*_{\alpha\beta} \quad (12)$$

The ShAF circuit control method is then developed and modelled in Figure 3 using Equations 1 through 12.

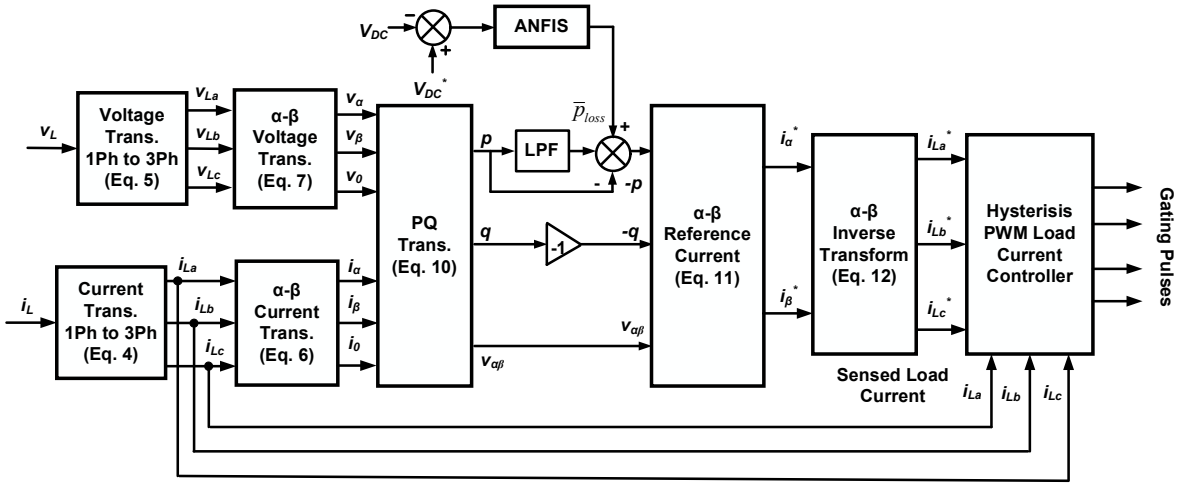

Figure 3. Single-phase ShAF control scheme using p-q theory

2.3. Fuzzy-Sugeno Control Design

Fuzzy logic control has two effects, namely the error value (e) and the delta error (Δe). This control model requires a degree of membership, IF-THEN activities, and a knowledge base. Fuzzy has a sequence in creating the central functional block system, namely the Knowledge Base, Fuzzification, Inference Mechanism, and Defuzzification. The knowledge base consists of a database and a rule base. The database consists of input and output membership functions, providing information for the appropriate fuzzification operations, inference mechanisms, and defuzzification. The rule base consists of a set of linguistic rules that relate fuzzy input variables to the desired control action. Figure 4 shows the fuzzy logic control flow chart using the Sugeno fuzzy inference system, which is hereinafter referred to in this paper as Fuzzy-Sugeno.

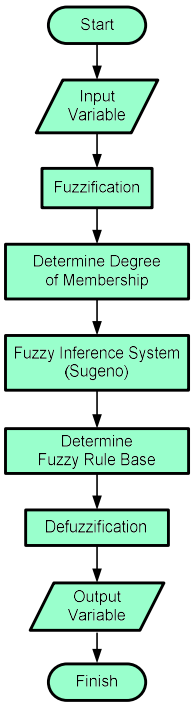

Figure 4. Flowchart of fuzzy logic control using FIS-Sugeno

This research uses two input variables $V_{DC-error}$ and $\Delta V_{DC-error}$ as well as $\bar{p}_{loss}$ as output variables. The method used in the fuzzy inference system is the Fuzzy Sugeno method. The Fuzzy Sugeno method uses a singleton MF, which has a membership degree of 1 for single crisp values and 0 for other crisp values. With such an MF model configuration, Fuzzy Sugeno produces a faster processing time because it has a weighted average to replace the defuzzification phase in Fuzzy Mamdani which requires a relatively long simulation time [50]. The value of two input variables and one output variable in each membership function is divided

into seven linguistic variable chips. Crips input variables used in $V_{DC-error}$ and $\Delta V_{DC-error}$ are NB (Negative Big), NS (Negative Medium), NM (Negative Small), Z (Zero), PS (Positive Small), PM (Positive Medium) and PB (Positive Big) with fuzzy rule base are shown in Table 2. Crips of input variables are triangular and trapezoidal memberships functions (MFs) with membership function limits between -650 to 650 In contrast to the input variable crips, the output crips variable is $\bar{p}_{loss}$ in the form of two different constant values [0,1] with a membership function limit between -100 to 100. The input variable crips and the output variable crips both have the same linguistic variable. Fuzzy Sugeno MFs of two input variables and one output variable are shown in Figure 5, Figure 6, and Figure 7, respectively.

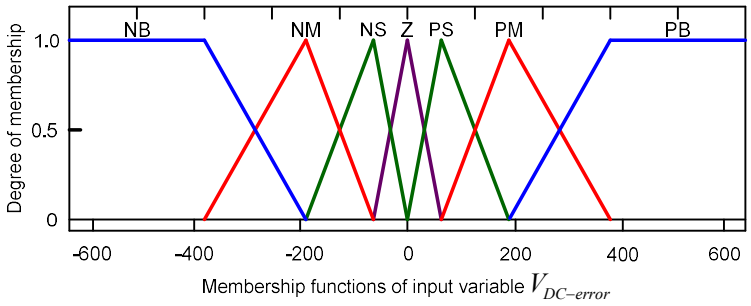

Figure 5. Input MFs of $V_{DC-error}$

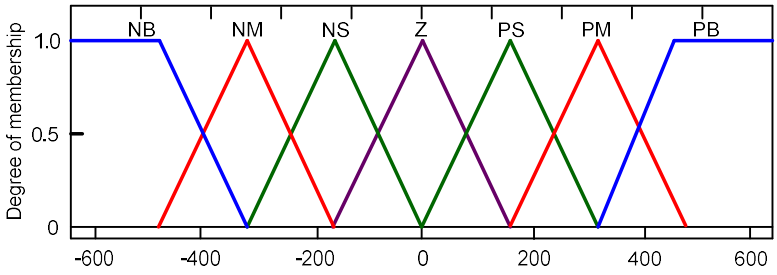

Figure 6. Input MFs of $\Delta V_{DC-error}$

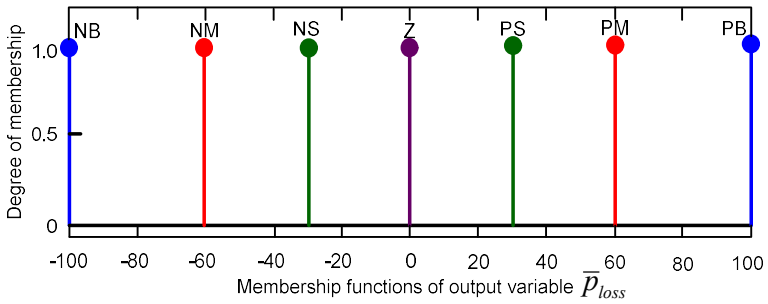

Figure 7. Output MFs of $\bar{p}_{loss}$

Table 2. Fuzzy Rule Base

$V_{DC-error}$ / $\Delta V_{DC-error}$	NB	NM	NS	Z	PS	PM	PB
PB	Z	PS	PS	PM	PM	PB	PB
PM	NS	Z	PS	PS	PM	PM	PB
PS	NS	NS	Z	PS	PS	PM	PM
Z	NM	NS	NS	Z	PS	PS	PM
NS	NM	NM	NS	NS	Z	PS	PS
NM	NB	NM	NM	NS	NS	Z	PS
NB	NB	NB	NM	NM	NS	NS	Z

2.4. ANFIS Control Design

ANFIS combines fuzzy logic control and artificial neural networks (ANN). The adaptive fuzzy technique modifies the fuzzy relationship and is generated from a representative sample of mathematics. The fuzzy rules that are unsure can be improved using the training data. Figure 8 depicts the ANFIS control architecture.

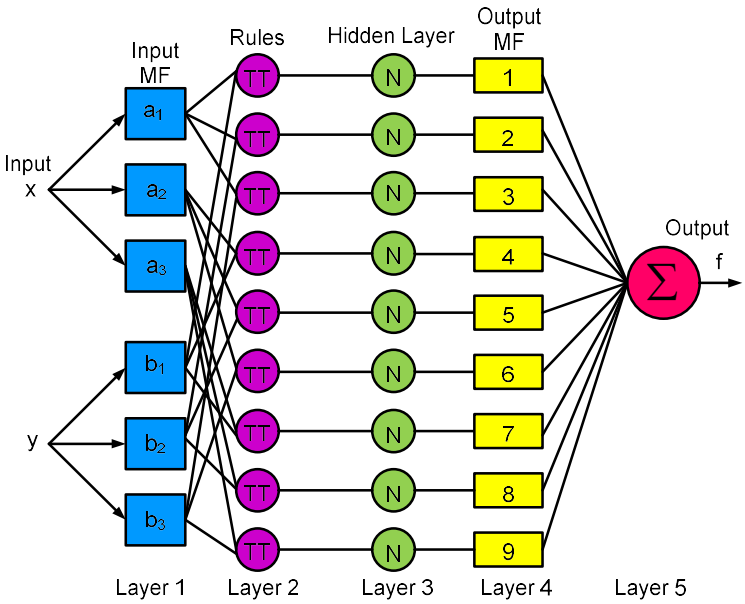

Figure 8. Architecture of ANFIS control

When dealing with higher processing skills and the subject of intelligence, fuzzy sets are regarded as beneficial. The NN block receives fuzzy input and triangle membership functions. The NN block is connected to a FIS and consists of a rule base. To train FIS, the back propagation (BP) method was applied. The feed-forward NN was trained using the BP learning method. Mamdani and Sugeno are the two FIS models most frequently utilized. Because (i) its membership function (MF) is linear or constant, (ii) it is more computationally efficient than the Mamdani type, and (iii) it may be trained using real data rather than historical data, which is more vulnerable to expert systems. Figure 9 displays the flowchart for ANFIS training.

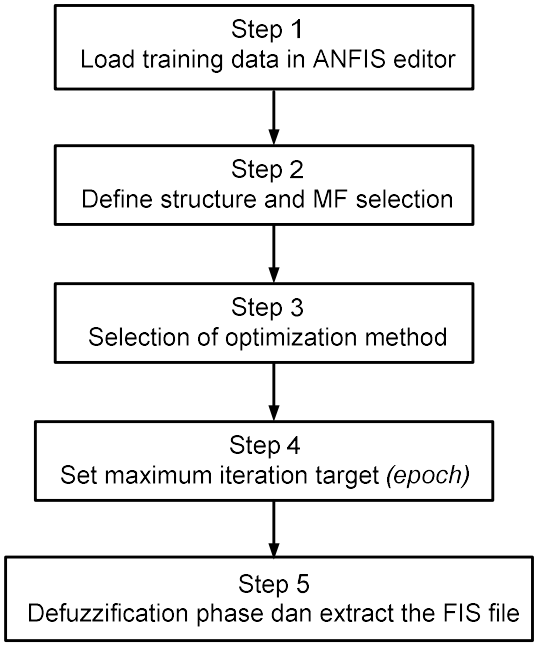

Figure 9. Flowchart of ANFIS training

A fuzzy neural network, also known as a neuro-fuzzy system, utilizes the neural network approximation technique to learn the characteristics of a fuzzy system, including fuzzy sets and fuzzy rules. There are some parallels between fuzzy systems and neural networks. Both can be used to address the given problem if there is no mathematical model for it (eg, pattern recognition, regression, or density estimation). The benefits and drawbacks of neural networks and fuzzy systems are lost mainly when the two concepts are combined. Figure 10 illustrates the model of ANFIS control employed in this study.

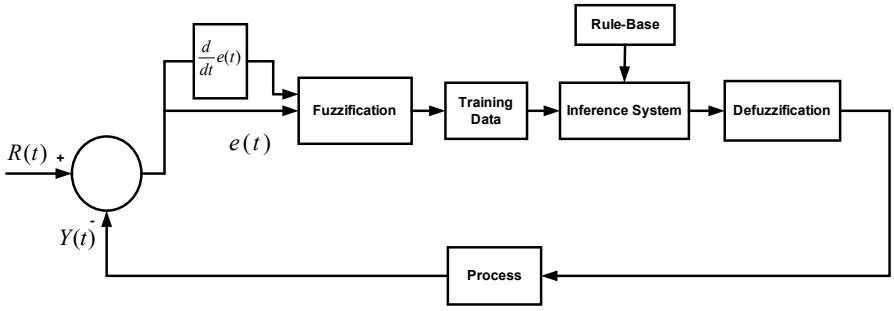

Figure 10. Model of ANFIS control

Figure 10 shows that the error value $e(t)$ is obtained from $e(t) = Y(t) - R(t)$ where $Y(t)$ and $R(t)$ are the output and input values of the system as a reference. Initially, the error value $e(t)$ and the change in error value (delta error $e(t)$) will be converted to fuzzy variable values in the fuzzification block. Same with PI and Fuzzy Sugeno control, the error value $e(t)$ and the value of delta error $e(t)$ are $V_{DC-error}$ and $\Delta V_{DC-error}$, respectively. After the fuzzification process, the output value of the fuzzification stage will be trained first by using the ANFIS editor by typing the command "anfisedit" in the Matlab command prompt, after that the fuzzification results that have been trained will enter the Inference Mechanism process by considering the rule base and membership function which automatically created after doing data training. After that, the defuzzification stage is processed to convert the fuzzy variable into its final output form in this system, which is then processed by the PWM inverter block to generate pulses. The data that was previously trained is then entered into the ANFIS editor window, where the results are shown in Figure 11. Figure 12 shows the learning construction of ANFIS.

Figure 11. Results of training data using the ANFIS editor window

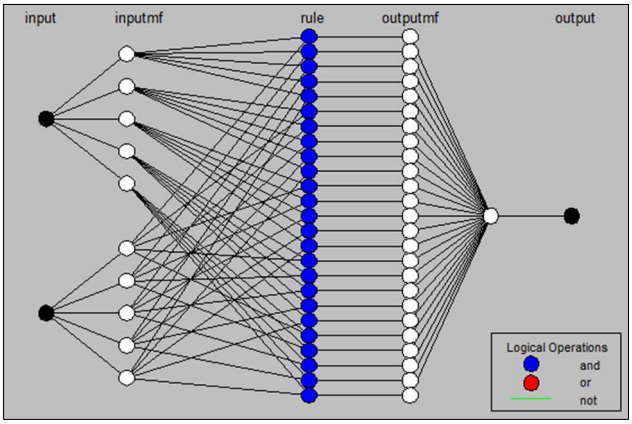

Figure 12. Structure of ANFIS input and output MFs

The structure of the ANFIS input and output control MFs used in this study is shown in Figure 12. The input model of the ANFIS training data obtained is derived from the reference and previous data calculations.

After the data training process is carried out, the MF model formed on the ANFIS control structure is then shown in Figure 13.

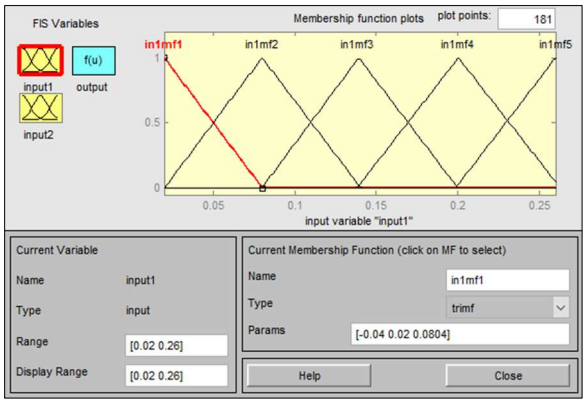

Figure 13. MFs of input variable 1 ($V_{DC-error}$)

Figure 13 is the MF input variable 1 ($V_{DC-error}$) that is formed after data training is performed on the ANFIS controller. Five linguistic variables utilize the triangular membership function (TRIMF) type in the range of values from 0 to 0.25.

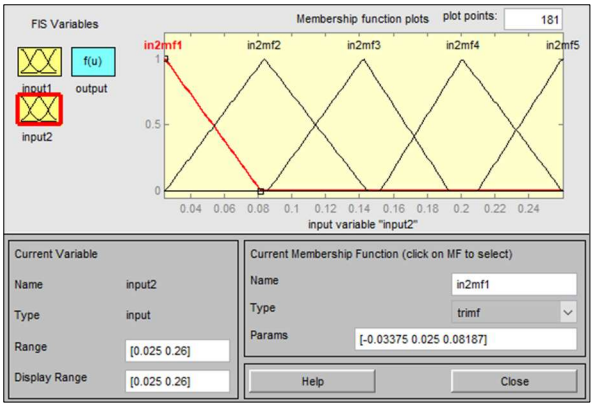

Figure 14. MFs of input variable 2 ($\Delta V_{DC-error}$)

Figure 14 shows the ANFIS control membership function value at input 2 ($\Delta V_{DC-error}$) totaling five MFs. MFs delta error has an interval limit equal to the input variable 1 ($\Delta V_{DC-error}$) using triangular (trimf) MFs type with an interval value between 0 and 0.25.

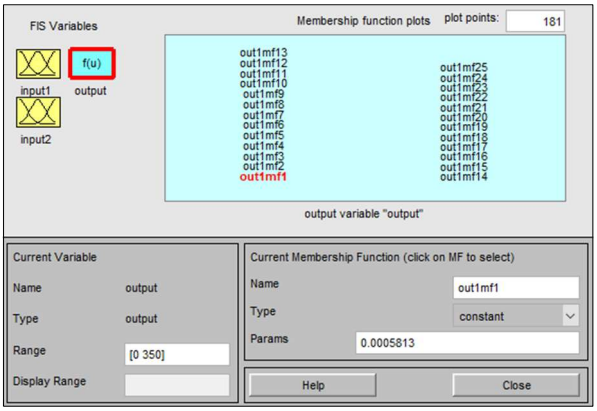

Figure 15. MFs of output variable ($\bar{p}_{loss}$)

Figure 15 shows the MF of the output variable for ANFIS ($\bar{p}_{loss}$). In contrast to fuzzy logic control, which employs the Mamdani method for its output, the FIS method used in ANFIS is the Fuzzy Sugeno method. The output value in this method is obtained by setting the rule base based on linguistic variables, and the range of

input variables 1 and 2, each of which is five variables. The number of MFs is 25, where the value is obtained from the MF input one and MF input 2, which the rule editor automatically generates.

3. Results and Discussions

3.1 Model Simulation

The proposed model is determined using three circuit models as shown in Figure 2a, Figure 2b, and Figure 3c. Three circuit models are proposed, namely without ShAF, using ShAF, and using ShAF-PV in a single-phase system connected to a non-linear load. In the system using ShAF and ShAF-PV, each uses PI, FS, and ANFIS-based ShAF control so that the total model used in this study is seven cases. The seven case models are Case 1 (without ShAF), Case 2 (using ShAF-PI), Case 3 (using ShAF-FS), Case 4 (using ShAF-ANFIS), Case 5 (using ShAF-PV-PI), Case 6 (using ShAF-PV-FS), and Case 7 (using ShAF-PV-ANFIS). Single-phase CB1 is used to connect ShAF to the system, while CB2 is used to connect PV to ShAF.

By using MATLAB Simulink, each model combination is executed according to the desired case to get the curve of the source voltage (V_S), load voltage (V_L), source current (I_S), load current (I_L), compensation current (I_C), DC-link voltage (V_{DC}), and PV voltage(V_{PV}). Based on this curve, the magnitude value of the source voltage (V_S), load voltage (V_L), source current (I_S), load current (I_L), compensation current (I_C), DC-link voltage (V_{DC}), and PV voltage(V_{PV}). Furthermore, the value of total harmonic distortion or THD V_S, THD V_L, THD I_S, and THD I_L is also determined based on a number of curves that have been plotted previously. Finally, the next step is to determine the active load power (P_L), source reactive power (Q_S), and ShAF reactive power (Q_{Sh}) to determine the contribution of reactive power in a single-phase system using ShAF and ANFIS control supplied by PV generators. Measurements were carried out in one cycle starting from t = 0.25 seconds with a total simulation time of t = 0.5 seconds. The curves of the source voltage (V_S), load voltage (V_L), source current (I_S), load current (I_L), compensation current (I_C), DC-link voltage (V_{DC}), and PV voltage (V_{PV}) in three model configurations are shown in Figure 16, Figure 17, and Figure 18, respectively. While the magnitude values and nominal values of THD V_S, THD V_L, THD I_S, dan THD I_L, are shown in Tables 2 and 3, respectively.

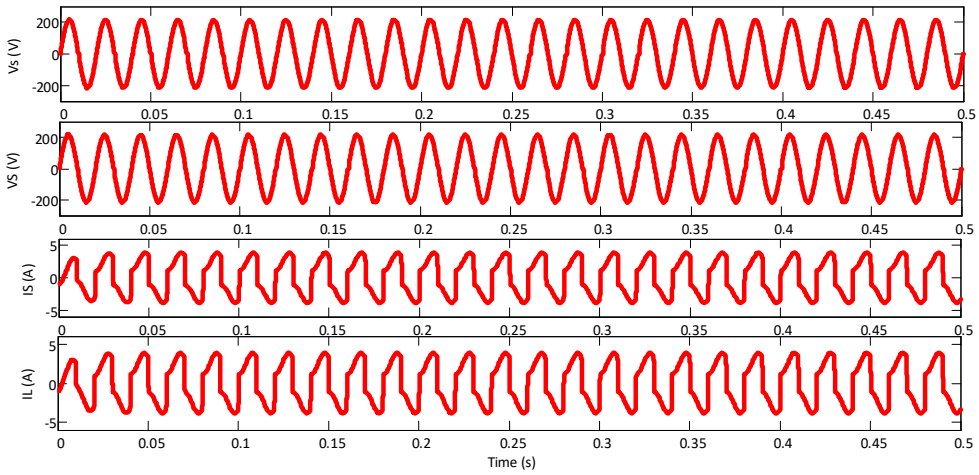

Figure 16. Performance of V_S, V_L, I_S, dan I_L on a single-phase system without ShAF (Case 1)

Figure 16 shows that at t=0.25 sec of the total simulation time of t=0.5 sec, a single-phase system without ShAF (Case 1) produces a magnitude and THD of source voltage (V_S) of 220 V and 1.76%, respectively. This value is equal to the magnitude and THD of the load voltage (V_L). Because it does not have a ShAF compensation circuit, the magnitude and THD values of the source current (I_S) and load current (I_L) each gives the same result of 3,851 A and 33.90%, respectively.

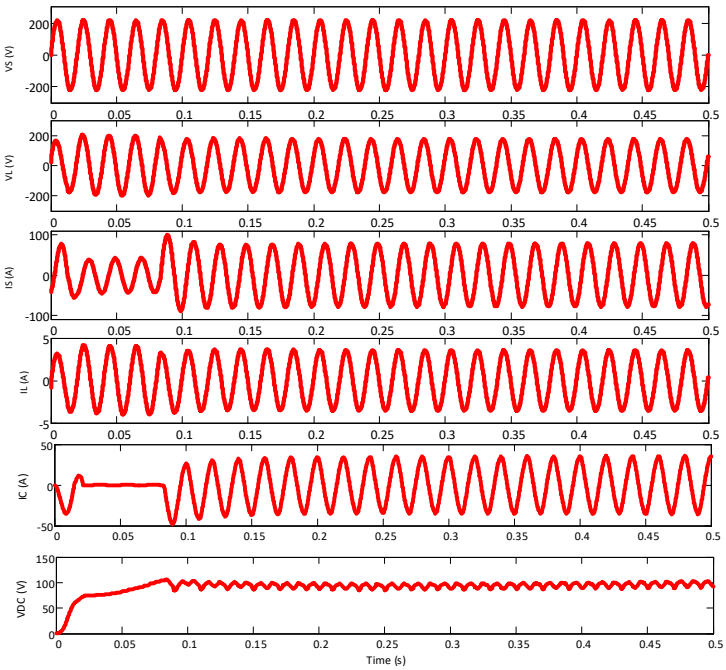

Figure 17. Performance of V_S, V_L, I_S, I_L and V_{DC} on a single-phase system with ShAF-ANFIS (Case 4)

Figure 17 shows that at t = 0.25 sec, a single-phase system with ShAF-ANFIS (Case 4) produces a magnitude and THD of the source voltage of 220 V and 9.74%, respectively, within the total simulation time of t = 0.5 sec. This value is equal to the magnitude and THD of the load voltage (V_L). In this model, it injects a shunt compensation current (I_C) of 24.68 A and a THD of 15.03% in opposite phase to reduce the THD of the source current to 2.91% compared to the THD of the load current of 31.76%.

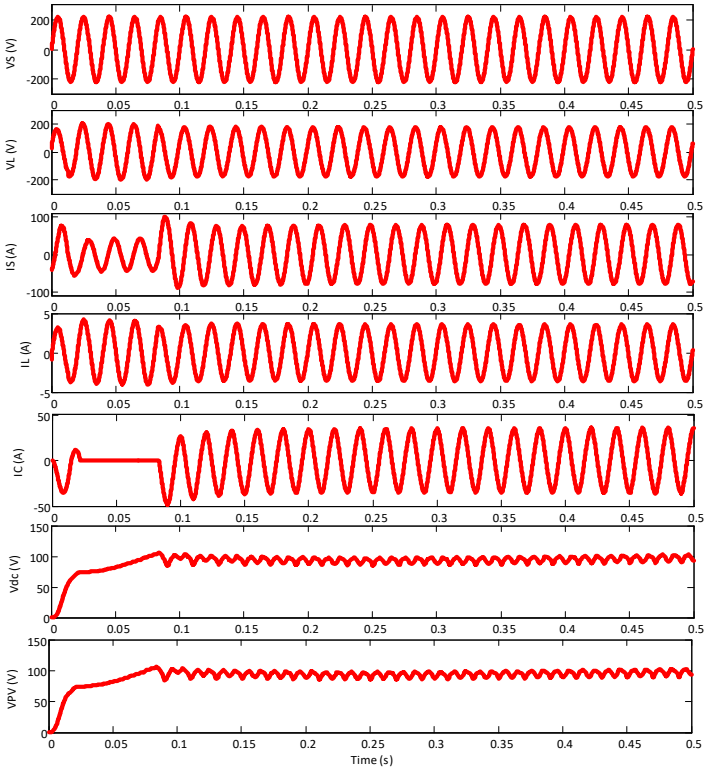

Figure 18. Performance of V_S, V_L, I_S, I_L, V_{DC}, and V_{PV} on a single-phase system with ShAF-PV-ANFIS (Case 7)

Figure 18 shows that at t=0.25 sec of the total simulation time of t=0.5 sec, a single-phase system with ShAF-PV-ANFIS-PV (Case 7) produces a magnitude and THD of source voltage (V_S) of 220 V and 1.76%. This value is the same as the magnitude and THD of the load voltage (V_L). In this model, the ShAF-PV-ANFIS circuit is capable of injecting a shunt compensation current (I_C) of 24.78 A and a THD of 5.03% in opposite phase to reduce the THD of the source current (I_S) to 1.54% compared to the THD of the load current (I_L) of 33.54%.

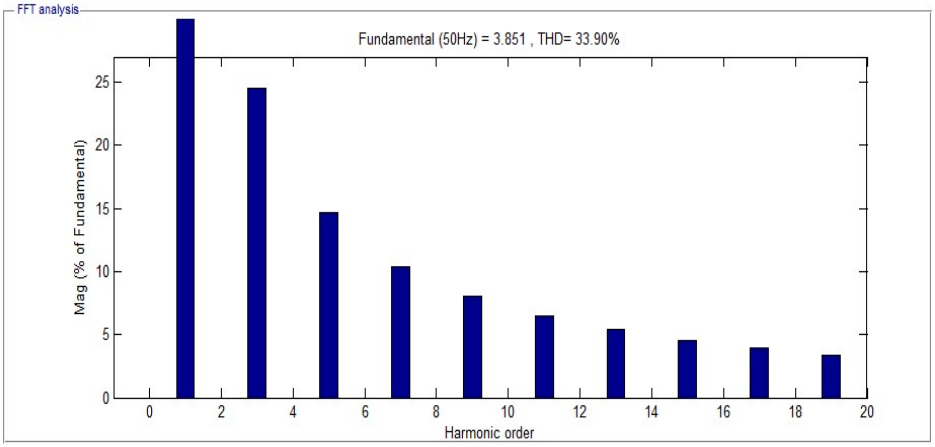

Figure 19. Harmonic spectra of source current on a single-phase system system without ShAF (Case 1)

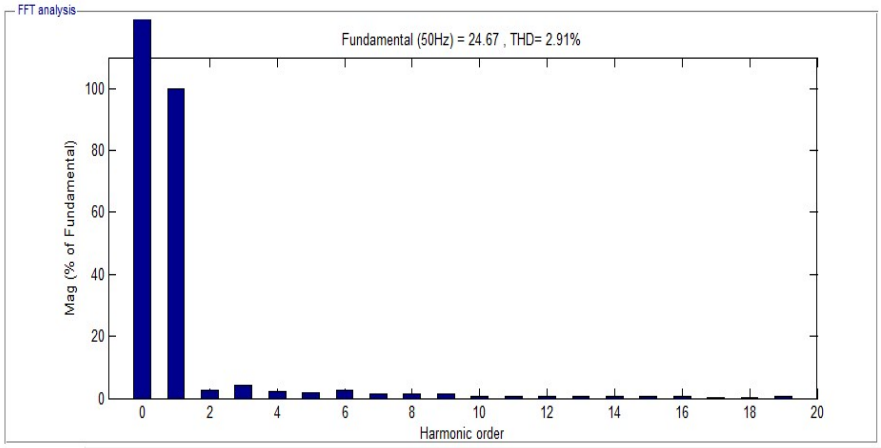

Figure 20. Harmonic spectra of source current on a single-phase system with ShAF-ANFIS (Case 4)

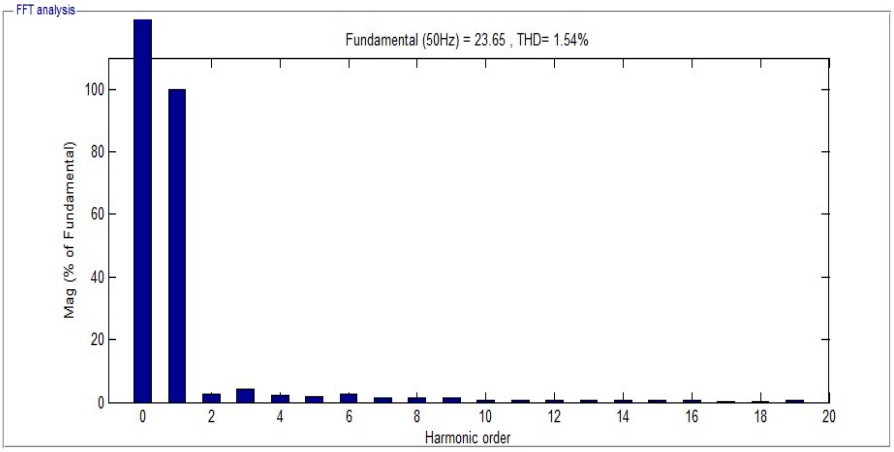

Figure 21. Harmonic spectra of source current on a single-phase system with ShAF-PV-ANFIS (Case 7)

Figure 19 shows that at t=0.25 sec of the total simulation time of t=0.5 sec, a single-phase system without ShAF (Case 1) is able to produce magnitude and THD values of source current (I_S) of 3,851 A and 33.90%, respectively. Since it does not have a ShAF compensation circuit, it is equal to the magnitude and THD of the load current (I_L). Figure 20 shows a single-phase system with ShAF-ANFIS (Case 4)-capable of producing a source current THD magnitude value (I_S) of 24.67 A and 2.91%, respectively. Figure 21 shows a single-phase system with ShAF-ANFIS (Case 7)-capable of producing magnitude and THD values of source current (I_S) of 23.65 A and 1.54%, respectively. In the same procedure, the magnitude and THD values for the source voltage (V_S) load voltage (V_L) source current (I_S), and load current (I_L) for the configuration of Case 2, Case 3, Case 5, and Case 6 are simulated dan presented entirely in Tables 3 and 4.

Table 3. Current and Voltage Magnitude Values in Seven Proposed Case

Case	Model	I_S (A)	I_L (A)	I_C (A)	V_S (V)	V_L (V)
1	Without ShAF	3.851	3.851	0	220	220
2	With ShAF-PI	24.42	4.197	22.93	220	220
3	With ShAF-FS	25.34	5.43	23.47	220	220
4	With ShAF-ANFIS	24.67	4.34	24.68	220	220
5	With ShAF-PV-PI	23.43	4.43	22.56	220	220
6	With ShAF-PV-FS	24.42	4.76	23.90	220	220
7	With ShAF-PV-ANFIS	23.65	4.25	24.78	220	220

Table 4. Current and Voltage THD Values in Seven Proposed Cases

Case	Model	$THD\ I_S$ (%)	$THD\ I_L$ (%)	$THD\ I_C$ (%)	$THD\ V_S$ (%)	$THD\ V_L$ (%)
1	Without ShAF	33.90	33.90	0	1.76	1.76
2	With ShAF-PI	3.12	35.19	3.680	9.74	9.74
3	With ShAF-FS	3.70	31.12	5.990	8.17	8.17
4	With ShAF-ANFIS	2.91	31.76	15.03	9.74	9.74
5	With ShAF-PV-PI	2.91	33.16	2.830	8.17	8.17
6	With ShAF-PV-FS	2.13	34.09	16.14	1.76	1.76
7	With ShAF-PV-ANFIS	1.54	33.54	5.030	1.76	1.76

Performance of THD Source Current using PI, Fuzzy Sugeno and ANFIS control under without ShAF, with ShAF, and with ShAF-PV is shown in Figure 22.

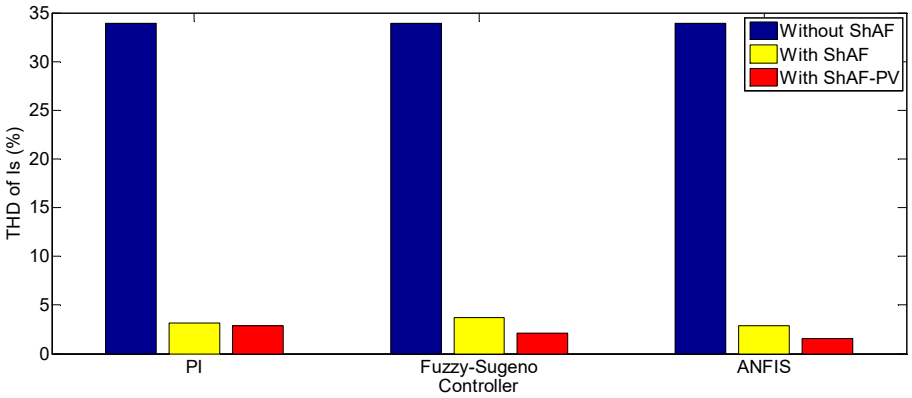

Figure 22. Performance of THD Source Current using PI, Fuzzy Sugeno and ANFIS control under conditions: (a) Without ShAF, (b) With ShAF, and (c) With ShAF-PV

Table 4 and Figure 9 show that a single-phase system without using ShAF produces a source current THD value (I_S) of 33.90%. The use of PI control using ShAF and ShAF-PV resulted in source current THD values (I_S) of 3.21% and 2.91%, respectively. The use of Fuzzy-Sugeno control using ShAF and ShAF-PV produces the THD value of the source current (I_S) of 3.70% and 2.91%, respectively. Meanwhile, the use of ANFIS control using ShAF and ShAF-PV is able to produce THD values of source current (I_S) of 2.91% and 1.54%, respectively. These results indicate that the use of ShAF in a single-phase system connected to a non-linear load is able to significantly reduce the THD of the source current (I_S) compared to a system without using ShAF. The single-phase ShAF circuit is capable of injecting compensating current into the load bus so as to successfully reduce the current harmonic content on the source bus under IEEE-519 requirements. The ShAF circuit using ANFIS control supplied by PV is also able to produce the best performance because it is able to produce the lowest source current THD (I_S) compared to the ShAF configuration without and with PV injection based on Fuzzy-Sugeno and PI control.

3.2 Power Transfer Analysis

The study also conducted a power transfer analysis on the single-phase ANFIS control model configuration using ShAF, both with and without PV injection. The analysis includes the examination of active load power, source reactive power, and ShAF reactive power transfer on systems using ShAF with and without PV injection.

3.2.1.Power Transfer Using Single-Phase ShAF Without PV Injection

Figure 23 shows the power transfer simulation of the load active power (P_{Load}), source reactive power (Q_{Source}), and ShAF reactive power (Q_{ShAF}) on a system using ShAF without PV injection. Simulations were carried out in two conditions, namely a single-phase system before and after being connected to the ShAF circuit at a time duration of ($t = 0.0\ to\ 0.2$ sec) and ($t = 0.2\ to\ 0.5$ sec) . The nominal power transfer measurements were carried out at $t = 0.0\ sec$ and $t = 0.3\ sec$, respectively. The simulation results under these conditions are then presented fully in Table 3.

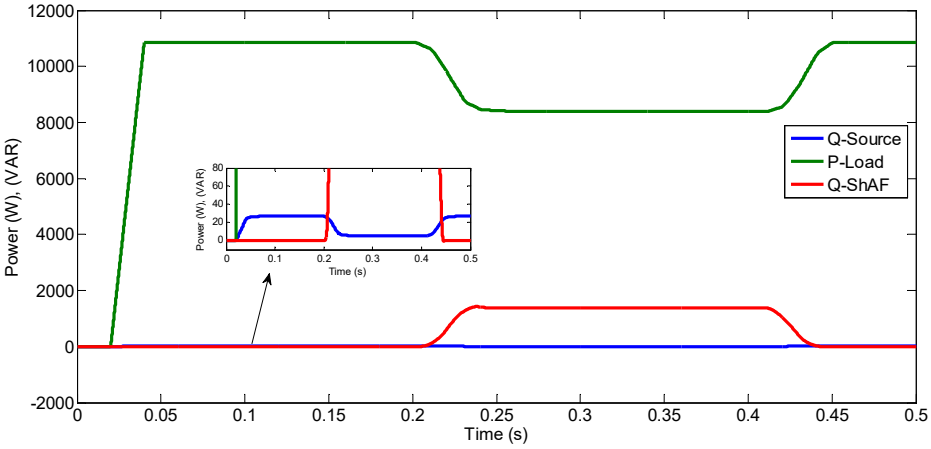

Figure 23. Transfer of load active power, source reactive power, and ShAF reactive power in a system using ShAF without PV injection

Table 5. Transfer of load active power, source reactive power, and ShAF reactive power on single-phase systems using ShAF without PV injection

Control Method	Before connected ShAF			After connected ShAF		
	0.1 *sec*			0.3 *sec*		
	P_{Load} (W)	Q_{Source} (VAR)	Q_{ShAF} (VAR)	P_{Load} (W)	Q_{Source} (VAR)	Q_{ShAF} (VAR)
PI	10850	26	0	9300	1,7	1400
Fuzzy Sugeno	10850	26	0	9240	2	1420
ANFIS	10850	26	0	9200	2,3	1500

Table 5 shows that in a single-phase system, before being connected, ShAF ($t = 0.1$ sec) produces load active power (P_{Load}), source reactive power (Q_{Source}) , and ShAF reactive power (Q_{ShAF}) are 10850 W, 26 VAR, and 0 VAR, respectively. The use of PI control in a single-phase system after connecting the ShAF ($t = 0.3$ sec) can reduce the load active power and source reactive power to 9300 W and 1.7 VAR, respectively and increase the ShAF reactive power to 1400 VAR. The use of ShAF with Fuzzy Sugeno control in a single-phase system ($t = 0.3$ sec) is able to reduce the active load and source reactive power to 9240 W and 2 VAR, respectively and increase the ShAF reactive power to 1420 VAR. Figure 23 shows that the use of ShAF with ANFIS control on a single-phase system ($t = 0.3$ sec) can reduce the active load and source reactive power to 9200 W and 2.3 VAR, respectively and increase the ShAF reactive power to 1500 VAR. The use of ShAF on a single-phase system with ANFIS control produces the lowest reactive power reduction of 9200 W, compared to PI and Fuzzy Sugeno controls of 9300 W and 9240 W, respectively. The use of ShAF in a single-phase system with ANFIS control enables the reactive power of ShAF to reach its highest value of 1500 VAR, surpassing the values of 1400 VAR and 1420 VAR achieved by PI and Fuzzy Sugeno controls, respectively.

3.2.2.Power Transfer Using Single-Phase ShAF with PV Injection

Figure 24 shows the power transfer simulation of the load active power (P_{Load}), source reactive power (Q_{Source}) and ShAF reactive power (Q_{ShAF}) on a system using ShAF with PV injection. Similar to the ShAF procedure without PV injection, the simulation was carried out under two conditions, namely a single-phase system before and after connecting to the ShAF-PV circuit at time durations ($t = 0.0\ to\ 0.2$ sec) and ($t = 0.2\ to\ 0.5$ sec). The nominal power transfer measurements are performed at $t = 0.1\ sec$ and at $t = 0.3\ sec$, respectively. The simulation results under these conditions are then presented fully in Table 6.

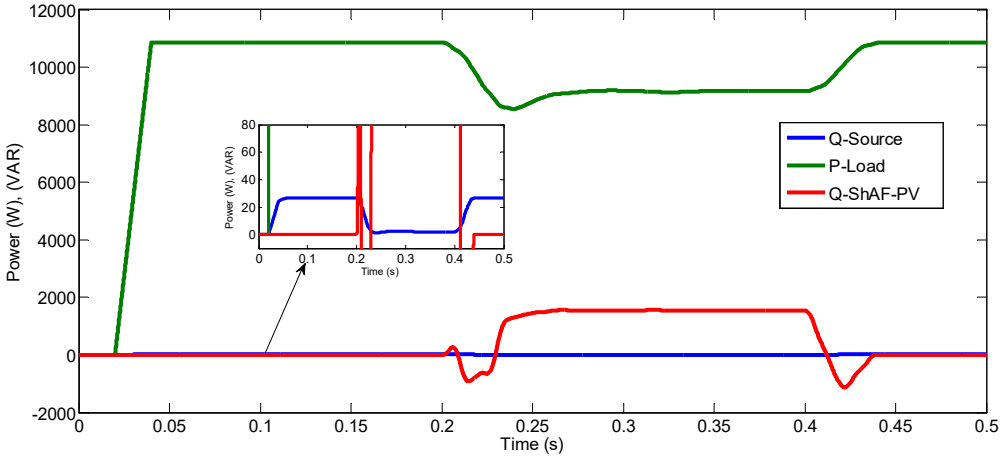

Figure 24. Transfer of load active power, source reactive power, and ShAF reactive power in a system using ShAF with PV injection

Table 6. Transfer of load active power, source reactive power, and ShAF reactive power in a system using ShAF with PV injection

Control Method	Before connected ShAF-PV			After connected ShAF-PV		
	0.1 *sec*			0.3 *sec*		
	P_{Load} (W)	Q_{Source} (VAR)	Q_{ShAF} (VAR)	P_{Load} (W)	Q_{Source} (VAR)	Q_{ShAF} VAR)
PI	10850	26	0	9300	1.9	1430
Fuzzy Sugeno	10850	26	0	9240	2,3	1470
ANFIS	10850	26	0	9200	2,5	1550

Table 5 and Table 6 show that the single-phase system before being connected to ShAF or ShAF-PV ($t = 0.1\ sec$) produces load active power (P_{Load}), source reactive power (Q_{Source}) and ShAF reactive power (Q_{ShAF}) of 10850 W, 26 VAR, and 0 VAR, respectively. The use of PI control in a single-phase system after connecting the ShAF-PV ($t = 0.3\ sec$) was able to reduce the load active power and source reactive power to 9300 W and 1.9 VAR, respectively and increase the ShAF reactive power to 1430 VAR. The use of ShAF-PV with Fuzzy Sugeno control on a single-phase system ($t = 0.1\ sec$) is able to reduce the active load and source reactive power to 9240 W and 2.3 VAR, respectively and increase the ShAF reactive power to 1470 VAR. Figure 24 shows that the use of ShAF-PV with ANFIS control in a single-phase system ($t = 0.1\ sec$) can reduce the active load and source reactive power to 9200 W and 2.5 VAR, respectively, and increase the ShAF reactive power to 1550 VAR. Similar to ShAF, the implementation of ShAF-PV on a single-phase system with ANFIS control produces the lowest reactive power reduction of 9200 W, compared to PI and Fuzzy Sugeno controls of 9300 W and 9240 W, respectively. Similar to ShAF, the implementation of ShAF-PV, a single-phase system with ANFIS control, was able to increase the ShAF reactive power to a maximum of 1550 VAR, compared to the PI and Fuzzy Sugeno controls, which achieved 1430 VAR and 1420 VAR, respectively. The difference is that a single-phase system using ShAF-PV, which employs three control methods, can produce a higher has a higher ShAF reactive power than a system connected only to ShAF. Table 5 also shows that a single-phase system using ShAF-PV with ANFIS control can inject the most immense ShAF reactive power compared to a system without PV injection.

3.2.3.Single Phase ShAF Reactive Power Compensation

Figure 25 shows the comparison of ShAF reactive power without and using PV injection on the three proposed control models at $t = 0.3$ sec.

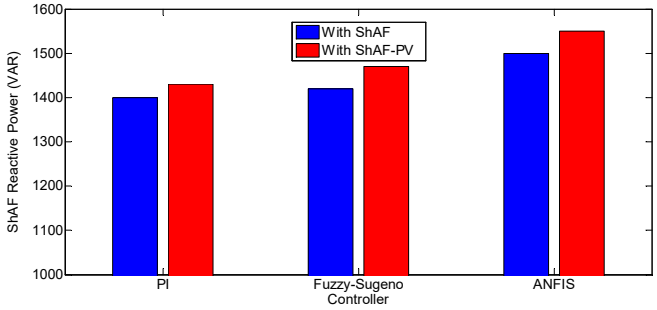

Figure 25. Comparison of ShAF reactive power with PI, Fuzzy Sugeno, and ANFIS control using ShAF and ShAF-PV.

Figure 25 shows a single-phase system connected to a non-linear load, which is connected to ShAF and ShAF-PV $t = 0.3$ sec) using a PI controller), producing a ShAF reactive power of 1400 VAR and 1430 VAR, respectively. The use of Fuzzy-Sugeno control on ShAF and ShAF-PV ($t = 0.3$ sec) resulted in 1420 VAR and 1470 VAR, respectively. Meanwhile, the use of ANFIS control on ShAF and ShAF-PV ($t = 0.3$ sec) resulted in 1500 VAR and 1550 VAR, respectively. Thus, among the three proposed control models, a single-phase system using ShAF with PV injection and ANFIS control can inject the largest reactive power compared to ShAF without PV injection. Increasing the reactive power of the ShAF circuit through PV injection will further compensate for the reactive power, resulting in a significant decrease in the source's reactive power.

4. Conclusion

A combination of single-phase ShAF with PV panels has been proposed to reduce source current harmonics and compensate for reactive power in a single-phase distribution system with a 220 V, 50 Hz voltage, connected to a non-linear load, utilizing ANFIS control. The ShAF-PV circuit with ANFIS control can produce the best performance because it can produce the lowest THD of source current. The single-phase system using ShAF-PV with ANFIS control is also capable of injecting the most considerable reactive power compared to the ShAF and ShAF-PV configurations with PI and Fuzzy-Sugeno control. The increase in reactive power in the ShAF-PV further compensates for the reactive power, thereby significantly suppressing the source reactive power. The ShAF and ShAF-PV circuits with ANFIS control still produce a slightly higher source reactive power value than the two models of the same circuit using PI and Fuzzy Sugeno controls, respectively. The use of ANFIS control with a constructive backpropagation NN training algorithm can be proposed to increase the accuracy of NN training on ANFIS, so that it is expected to be able to reduce the

source reactive power. Real-time implementation on hardware in the future is also needed to validate whether the proposed simulation method by the author can work in the real model.

ACKNOWLEDGEMENTS

The authors would like to thank the Institutions of Research and Community Service Universitas Bhayangkara Surabaya for supporting this research.

REFERENCES

[1] M. Duc, P. Bilík, & R. Martínek, "Enhancing Power Quality in Industry 4.0 Manufacturing Using the Multi-Criteria Selection Method," *IEEE Access*, vol. 12, pp. 63171-63198, 2024. https://doi.org/10.1109/access.2024.3388846.

[2] S. Das, A. Hota, H. Pandey, & B. Sahoo, "Industrial Power Quality Enhancement using Fuzzy Logic based Photovoltaic Integrated with Three Phase Shunt Hybrid Active Filter and Adaptive Controller," *Applied Soft Computing*, vol. 121, pp. 108762, 2022. https://doi.org/10.1016/j.asoc.2022.108762.

[3] M. Dellahi, H. Maker, A. Mouhsen, & E. Hernández, "Three-Phase Four Wire Shunt Active Power Filter Based on Simplified Backstepping Technique for DC Voltage Control," *RE&PQJ*, vol. 16, no. 5, 2024. https://doi.org/10.24084/repqj16.384.

[4] S. Mohsen, A. Ibrahim, Z. Elbarbary, & A. Omar, "Unified Power Quality Conditioner Using Recent Optimization Technique: A Case Study in Cairo Airport, Egypt," *Sustainability*, vol. 15, no. 4, pp. 3710, 2023. https://doi.org/10.3390/su15043710.

[5] S. Ouchen, M. Benbouzid, F. Blaabjerg, A. Betka, & H. Steinhart, "Direct Power Control of Shunt Active Power Filter Using Space Vector Modulation Based on Supertwisting Sliding Mode Control," *IEEE Journal of Emerging and Selected Topics in Power Electronics*, vol. 9, no. 3, pp. 3243-3253, 2021. https://doi.org/10.1109/jestpe.2020.3007900.

[6] Q. Li, B. Ren, Q. Li, D. Wang, W. Tang, J. Meng et al., "Virtual Inertial Control Strategy Based on Fuzzy Logic Algorithm for PMSG Wind Turbines to Enhance Frequency Stability," *Frontiers in Energy Research*, vol. 10, 2022. https://doi.org/10.3389/fenrg.2022.907770.

[7] J. Zhou, Y. Sun, S. Chen, & T. Lan, "A Fast Repetitive Control Strategy for a Power Conversion System," *Electronics*, vol. 13, no. 7, p. 1186, 2024. https://doi.org/10.3390/electronics13071186.

[8] A. Amerise, M. Mengoni, G. Rizzoli, L. Zarri, A. Tani, & D. Casadei, "Comparison of Three Voltage Saturation Algorithms in Shunt Active Power Filters with Selective Harmonic Control," *IEEE Transactions on Industry Applications*, vol. 56, no. 3, pp. 2762-2772, 2020. https://doi.org/10.1109/tia.2020.2972853.

[9] M. Ebrahim, S. Ward, M. El-Gohary, M. Mohamad, M. Eid, A. Alharbi et al., "AI-based Voltage and Power Quality Control of High-Penetration Grid-Connected Photovoltaic Power Plant," *Frontiers in Energy Research*, vol. 11, 2023. https://doi.org/10.3389/fenrg.2023.1178521.

[10] A. Mukhatov, N. Thao, & T. Duc, "Linear Quadratic Regulator and Fuzzy Control for Grid-Connected Photovoltaic Systems," *Energies*, vol. 15, no. 4, pp. 1286, 2022. https://doi.org/10.3390/en15041286.

[11] I. Mexis, G. Todeschini, & Z. Zhou, "Coordinated Control of Three Single–Phase BESS Inverters Using Local Measurements to Mitigate Voltage Unbalance," *IEEE Transactions on Energy Conversion*, vol. 37, no. 4, pp. 2941-2951, 2022. https://doi.org/10.1109/tec.2022.3202137.

[12] L. Li, T. Yang, Y. Yuan, & Z. Cai, "A Model Predictive Control Strategy Based on Energy Storage Grid-Connected Quasi-z-source Inverters," *IET Generation, Transmission & Distribution*, vol. 16, no. 17, pp. 3451-3461, 2022. https://doi.org/10.1049/gtd2.12534.

[13] B. Rao, P. Krishna, & V. Yarlagadda, "Mitigation of Photovoltaic Solar System Harmonics using Shunt Active Power Filter," *2020 Fourth International Conference on Computing Methodologies and Communication (ICCMC),* pp. 566-571, 2020. https://doi.org/10.1109/iccmc48092.2020.iccmc-000105.

[14] R. Boopathi and V. Indragandhi, "Solar Photovoltaic-Interfaced Shunt Active Power Filter Implementation for Power Quality Enhancement in Grid-Connected Systems," *International Journal of Circuit Theory and Applications*, vol. 51, no. 11, pp. 5305-5323, 2023. https://doi.org/10.1002/cta.3710.

[15] R. Kumar, H. Bansal, A. Gautam, O. Mahela, & B. Khan, "Experimental Investigations on Particle Swarm Optimization Based Control Algorithm for Shunt Active Power Filter to Enhance Electric Power Quality," *IEEE Access*, vol. 10, pp. 54878-54890, 2022. https://doi.org/10.1109/access.2022.3176732.

[16] M. AlRashidi, "Community Battery Storage Systems Planning for Voltage Regulation in Low Voltage Distribution Systems," *Applied Sciences*, vol. 12, no. 18, pp. 9083, 2022. https://doi.org/10.3390/app12189083.

[17] R. Kumar and H. Bansal, "Investigations on Shunt Active Power Filter in a PV-wind-FC based Hybrid Renewable Energy System to Improve Power Quality using Hardware-in-the-loop Testing Platform," *Electric Power Systems Research*, vol. 177, pp. 105957, 2019. https://doi.org/10.1016/j.epsr.2019.105957.

[18] X. Pan, L. Zhang, Y. Li, K. Li, & H. Huang, "Modulated Model Predictive Control with Branch and Band Scheme for Unbalanced Load Compensation by MMCC-STATCOM," *IEEE Transactions on Power Electronics*, vol. 37, no. 8, pp. 8948-8962, 2022. https://doi.org/10.1109/tpel.2022.3152407.

[19] R. Naidu and S. Meikandasivam, "Power Quality Enhancement in A Grid-Connected Hybrid System with Coordinated PQ Theory & Fractional Order PID controller in DPFC," *Sustainable Energy, Grids and Networks*, vol. 21, pp. 100317, 2020. https://doi.org/10.1016/j.segan.2020.100317.

[20] M. Constantinescu, M. Popescu, G. Subţirelu, & C. Toma, "Modelling, Simulation and Implementation on dSpace 1103 of the Direct Power Control in a Three-Phase Shunt Active Power Filter System," *Annals of the*

University of Craiova Electrical Engineering Series, vol. 47, pp. 69-75, 2023. https://doi.org/10.52846/aucee.2023.11.

[21] M. Alali, Z. Sabiri, Y. Shtessel, & J. Barbot, "Grid-Connected Shunt Active Photovoltaic Filter," *2020 IEEE 29th International Symposium on Industrial Electronics (ISIE)*, pp. 120-125, 2020. https://doi.org/10.1109/isie45063.2020.9152458.

[22] A. Ali, "Design and Simulation of A Shunt Active Power Filter for Grid Tied PV Generators for Low Voltage Distribution Network," *2020 11th International Renewable Energy Congress (IREC)*, pp. 1-5, 2020. https://doi.org/10.1109/irec48820.2020.9310441.

[23] A. Azzam-Jai and M. Ouassaid, "A Novel Neural Instantaneous Power Theory for A Shunt Active Power Filter Interfaced Solar Photovoltaic System," *2020 IEEE International Conference on Power Electronics, Drives and Energy Systems (PEDES)*, pp. 1-6, 2020. https://doi.org/10.1109/pedes49360.2020.9379789.

[24] S. Bagi, F. Kudchi, & S. Bagewadi, "Power Quality Improvement using a Shunt Active Power Filter for Grid Connected Photovoltaic Generation System," *2020 IEEE Bangalore Humanitarian Technology Conference (B-Htc)*, pp. 1-4, 2020. https://doi.org/10.1109/b-htc50970.2020.9298001.

[25] G. Goswami and P. Goswami, "Artificial Intelligence based PV-Fed Shunt Active Power Filter for IOT Applications," *2020 9th International Conference System Modeling and Advancement in Research Trends (SMART)*, pp. 163-168, 2020. https://doi.org/10.1109/smart50582.2020.9337063.

[26] C. Khomsi, M. Bouzid, G. Champenois, & K. Jelassi, "Improvement of the Current Quality of a Single-phase Photovoltaic System Connected to the Grid," *2020 20th International Conference on Sciences and Techniques of Automatic Control and Computer Engineering (STA)*, pp. 237-242, 2020. https://doi.org/10.1109/sta50679.2020.9329342.

[27] B. Marwa, H. Berriri, & M. Faouzi, "Shunt Active Power Filter Based on Artificial Neural Networks for Grid-Connected Photovoltaic System," *2020 17th International Multi-Conference on Systems, Signals & Devices (SSD)*, pp. 256-261, 2020. https://doi.org/10.1109/ssd49366.2020.9364225.

[28] S. Mukherjee, S. Mazumder, & S. Adhikary, "Harmonic Compensation for Nonlinear Loads Fed by Grid Connected Solar Inverters Using Active Power Filters," *2020 IEEE VLSI Device Circuit and System (VLSI DCS)*, pp. 1-6, 2020. https://doi.org/10.1109/vlsidcs47293.2020.9179882.

[29] S. Naqvi, S. Kumar, & B. Singh, "A PV-Battery System Operating in Islanded and Grid Connected Modes with Shunt Active Filter Capability," *2020 IEEE Industry Applications Society Annual Meeting*, pp. 1-8, 2020. https://doi.org/10.1109/ias44978.2020.9334847.

[30] S. Setiyono, S. A. Sudiro, & E. P. Wibowo, "Modeling and Analysis of Three-Phase Active Power Filter Integrated Photovoltaic as a Reactive Power Compensator Using the Simulink Matlab Tool," *2020 Fifth International Conference on Informatics and Computing (ICIC)*, pp. 1-8, 2020. https://doi.org/10.1109/icic50835.2020.9288527.

[31] K. Sharma and V. Sharma, "Single Phase Modeling and Harmonics Compensation of Standalone PV+SOFC System with SAPF," *2020 International Conference on Electronics and Sustainable Communication Systems (ICESC)*, pp. 979-983, 2020. https://doi.org/10.1109/icesc48915.2020.9155669.

[32] B. Rao, P. Krishna, & V. Yarlagadda, "Mitigation of Photovoltaic Solar System Harmonics using Shunt Active Power Filter," *2020 Fourth International Conference on Computing Methodologies and Communication (ICCMC)*, pp. 566-571, 2020. https://doi.org/10.1109/iccmc48092.2020.iccmc-000105.

[33] S. Agrawal, S. K. Vaishnav, A. Ajit, & R. K. Somani, "Active Power Filter for Harmonic Mitigation of Power Quality Issues in Grid Integrated Photovoltaic Generation System," *2020 7th International Conference on Signal Processing and Integrated Networks (SPIN)*, pp. 317-321, 2020. https://doi.org/10.1109/spin48934.2020.9070979.

[34] M. Musarrat, M. Islam, K. Muttaqi, & D. Sutanto, "Shunt Active DC Filter to Reduce the DC Link Ripple Current Caused by Power Converters to Improve the Lifetime of Aluminium Electrolytic Capacitor," *2020 IEEE Industry Applications Society Annual Meeting*, pp. 1-7, 2020. https://doi.org/10.1109/ias44978.2020.9334871.

[35] A. Mishra, S. Chauhan, P. Karuppanan, & M. Suryavanshi, "PV based Shunt Active Harmonic Filter for Power Quality improvement," *2021 International Conference on Computing, Communication, and Intelligent Systems (ICCCIS)*, pp. 905-910, 2021. https://doi.org/10.1109/icccis51004.2021.9397214.

[36] S. Echalih, A. Abouloifa, J. Janik, I. Lachkar, Z. Hekss, F. Chaoui et al., "Hybrid Controller with Fuzzy Logic Technique for Three Phase Half Bridge Interleaved Buck Shunt Active Power Filter," *IFAC-PapersOnLine*, vol. 53, no. 2, pp. 13418-13423, 2020. https://doi.org/10.1016/j.ifacol.2020.12.247.

[37] S. Echalih, A. Abouloifa, I. Lachkar, J. Guerrero, Z. Hekss, & F. Giri, "Hybrid Automation-Fuzzy Control of Single-Phase Dual Buck Half Bridge Shunt Active Power Filter for Shoot Through Elimination and Power Quality Improvement," *International Journal of Electrical Power & Energy Systems*, vol. 131, pp. 106986, 2021. https://doi.org/10.1016/j.ijepes.2021.106986.

[38] M. Fallah, J. Modarresi, H. Kojabadi, L. Chang, & J. Guerrero, "A Modified Indirect Extraction Method for A Single-Phase Shunt Active Power Filter with Smaller DC-Link Capacitor Size," *Sustainable Energy Technologies and Assessments*, vol. 45, pp. 101039, 2021. https://doi.org/10.1016/j.seta.2021.101039.

[39] A. Eltamaly and Z. Almutairi, "Synergistic Coordination Between PWM Inverters and DC-DC Converters for Power Quality Improvement of Three-Phase Grid-Connected PV Systems," Sustainability, vol. 17, no. 8, pp. 3748, 2025. https://doi.org/10.3390/su17083748.

[40] Z. Hekss, A. Abouloifa, J. Janik, I. Lachkar, S. Echalih, F. Chaoui et al., "Hybrid Automaton Control of Three Phase Reduced Switch Shunt Active Power Filter Connected Photovoltaic System," *IFAC-PapersOnLine*, vol. 53, no. 2, pp. 12847-12852, 2020. https://doi.org/10.1016/j.ifacol.2020.12.1986.
[41] Z. Hekss, A. Abouloifa, I. Lachkar, F. Giri, S. Echalih, & J. Guerrero, "Nonlinear Adaptive Control Design with Average Performance Analysis for Photovoltaic System Based on Half Bridge Shunt Active Power Filter," *International Journal of Electrical Power & Energy Systems*, vol. 125, pp. 106478, 2021. https://doi.org/10.1016/j.ijepes.2020.106478.
[42] M. J. Kumar and K.Varalakshmi, "PV-Based Shunt Active Power Filter for Improving Power Quality in Accordance with the P-Q Theory," *International Journal for Modern Trends in Science and Technology*, vol. 8, no. 6, pp. 372-381, 2022. http://dx.doi.org/10.46501/IJMTST0806065.
[43] P. Reddy, B. Gupta, & K. Sekhar, "Design and Implementation of Load Network Time Constant Computation Based Solar Active Power Filters Cum Injector for Industrial Loads/Grids," *IEEE Access*, vol. 12, pp. 19967-19982, 2024. https://doi.org/10.1109/access.2024.3361309.
[44] R. Boopathi and V. Indragandhi, "Experimental Investigations on Photovoltaic Interface Neutral Point Clamped Multilevel Inverter-Based Shunt Active Power Filter to Enhance Grid Power Quality," *IEEE Access*, vol. 12, pp. 74482-74498, 2024. https://doi.org/10.1109/access.2024.3405533.
[45] M. R. Fazal, M.A.E. Alali, T. Phulpin, R. L. Forestier, & C. Goasguen, "Design, Control and Loss Analysis of PV-based Shunt Active Filter for Improved Power Quality with Maximum PV Power Injection," *HAL Open Science*, pp. 1-6, 2024. https://doi.org/10.34746/epe2025-0270.
[46] S. Prakash, M. Alkhatib, H. Sindi, S. Alghamdi, R. Behera, & U. Muduli, "Adaptive Control for Shunt Active Power Filter under Stochastic Solar Photovoltaics Behavior," *IEEE Journal of Emerging and Selected Topics in Power Electronics*, vol. 13, no. 3, pp. 3673-3687, 2025. https://doi.org/10.1109/jestpe.2025.3525489.
[47] N. Karania, M. Alali, S. Gennaro, & J. Barbot, "Advanced High Switching-Frequency Cascaded H-Bridge Multilevel Inverter Based Shunt Active Filter for PV Generation: A Case Study," *IEEE Open Journal of Industry Applications*, vol. 6, pp. 262-280, 2025. https://doi.org/10.1109/ojia.2025.3563851.
[48] T. Thentral, K. Vijayakumar, S. Usha, R. Palanisamy, T. Babu, H. Alhelou et al., "Development of Control Techniques Using Modified Fuzzy Based SAPF for Power Quality Enhancement," *IEEE Access*, vol. 9, pp. 68396-68413, 2021. https://doi.org/10.1109/access.2021.3077450.
[49] A. Imam, R. Kumar, & Y. Al-Turki, "Modeling and Simulation of a PI Controlled Shunt Active Power Filter for Power Quality Enhancement Based on P-Q Theory," *Electronics*, vol. 9, no. 4, pp. 637, 2020. https://doi.org/10.3390/electronics9040637.
[50] A. Bengag, A. Bengag, & O. Moussaoui, "Intrusion Detection based on Fuzzy Logic for Wireless Body Area Networks: Review and Proposition," *Indonesian Journal of Electrical Engineering and Computer Science*, vol. 26, no. 2, pp. 1091, 2022. https://doi.org/10.11591/ijeecs.v26.i2.pp1091-1102.

BIOGRAPHIES OF AUTHORS

Anis Fitriani was born in Rembang Central Java Indonesia in 1999. Since 2017, she has studied and achieved a Bachelor's degree in Electrical Engineering at the Faculty of Engineering at Universitas Bhayangkara Surabaya in 2021. The author's area of expertise is active filter design using artificial intelligence systems. The author worked for a private company in the automation and electrical design field for high-level buildings from 2022-2023. Since 2024, the author has received an Engineering Scholarship from the Mainichi Shinbun to study the Japanese language for two years at First Study Osaka Japan. The author can be contacted at email: anisfitriani213@gmail.com.

Amirullah was born in Sampang, East Java, Indonesia on May 20, 1977. The author completed his Bachelor's degree (S1) in Electrical Engineering Power Systems Engineering in 2000 and his Master's degree (S2) in Electrical Engineering-Power Systems in 2008 from Universitas Brawijaya Malang and Institut Teknologi Sepuluh Nopember (ITS) Surabaya, respectively. Furthermore, the author completed his Doctoral degree (S3) in Electrical Engineering at ITS Surabaya in 2019. Since 2002, the author has been a lecturer and now associate professor in the Electrical Engineering Department, Faculty of Engineering, Universitas Bhayangkara Surabaya. The author has 21 publications in Scopus-indexed international journals with an h-index of 8. In Google Scholar, the author has 58 publications with an h-index of 8. His research interests include modelling and simulation of power distribution, power quality, harmonic mitigation, filter design/power factor correction, protection power systems, and renewable energy based on artificial intelligence. In 2016, the author followed a short course at the 9th Asian School of Renewable Energy, at Universiti Kebangsaan Malaysia-organized by the Solar Energy Research Institute in collaboration with UNESCO. Now, the author is a Board Member of The Indonesian Electrical Engineering Education Forum (FORTEI), Scientific Publication Division for the period of 2024-2026. The correspondence author can be contacted at email: amirullah@ubhara.ac.id.

Krischonme Bhumkittipich is a professor of electrical engineering at the Department of Electrical Engineering, Faculty of Engineering, Rajamangala University of Technology Thanyaburi (RMUTT) in Pathum Thani, Thailand. He holds a Doctor of Engineering (D.Eng.) degree in Electrical Engineering. His academic journey includes a SIEMENS scholarship for research on multilevel converters for power system applications at ISEA, RWTH-Aachen, Germany, from 2001 to 2003, and an assistant researcher position at the Asian Institute of Technology, Thailand, from 2006 to 2008. Since 1997, he has been a lecturer at RMUTT, advancing to Assistant Professor in 2010, Associate Professor in 2015, and Professor in 2024. He has held several administrative roles, including Assistant to the Dean in Academic Affairs, Vice Dean of Academic and Research Affairs, and Director of RMUTT Graduate School from 2014 to 2019. Currently, he serves as Vice President of Academic and Research Affairs at RMUTT. Dr. Bhumkittipich has authored over 100 publications, including books on topics such as "Mathematical Model of Power System Analysis," "Power System Quality," "Voltage Stability and Control," and "Impact of Electric Vehicle Loads on Power System Stability." His research interests encompass power system interconnection, operation, automation, dynamic stability, power electronics applications, power quality, electric vehicles, charging stations, and energy storage systems. He is a member of several professional organizations, including IEEE, IEE, and IEEJ, and actively participates in the IEEE Thailand section's PES Chapter and PELS/IAS Chapter. Dr. Bhumkittipich also advises numerous master's and doctoral students annually, contributing significantly to electrical engineering research. The correspondence author can be contacted at email: krischonme.b@en.rmutt.ac.th.